Title page

Metabolism of echinacoside, a good antioxidant, in rats: isolation and identification of its

biliary metabolites

Cunqin Jia, Haiming Shi, Wei Jin, Ke Zhang, Yong Jiang, Mingbo Zhao, Pengfei Tu

Department of Natural Medicines, School of Pharmaceutical Sciences, Peking University

Health Science Center, Beijing, P.R. China (C.J., W.J., K.Z., Y.J., M.Z., P.T.); and School of

Pharmacy, Shanghai Jiao Tong University, Shanghai, P.R. China (H.S.)

Running title page

Running title: Metabolism of echinacoside, a good antioxidant, in rats

Corresponding author: Pengfei Tu

Address: Department of Natural Medicines, School of Pharmaceutical Sciences, Peking University Health Science Center, No. 38 Xueyuan Road, Haidian District, Beijing 100083, P.R. China; phone/fax: +86-10-82802750; E-mail: pengfeitu@bjmu.edu.cn

The number of text pages: 15.

The number of tables: 3.

The number of figures: 2.

The number of references: 34.

The number of words in *Abstract*: 173.

The number of words in *introduction*: 352.

The number of words in *discussion*: 1042.

ABBREVIATIONS: ECH, echinacoside; PEGs, phenylethanoid glycosides; $T_{1/2\alpha}$, the half life of distribution; $T_{1/2\beta}$, the half life of elimination; CL, the clearance; NMR, nuclear magnetic resonance; *E*-caffeoyl, *trans*-3-(3, 4-dihydroxy-phenyl)-acrylic acid; HSQC, heteronuclear single-quantum correlation; HMBC, heteronuclear multiple-bond correlation; gCOSY, gradient-selected correlation spectroscopy; NOEDS, nuclear overhauser effect difference spectroscopy; NOESY, nuclear overhauser effect spectroscopy; HPLC, high-performance liquid chromatography; Me, methyl-; ESI, electrospray ionization; MS, mass spectrometry; COMT, catechol O-methyltransferase; UGT, UDP-glucuronosyltransferase; ST, sulfotransferase; UV, ultraviolet; IR, infrared; TFA,

trifluoroacetic acid; EDTA, ethylene diamine tetraacetic acid; NBT, nitro blue tetrazolium.

Abstract

Echinacoside (ECH), is one of the major active phenylethanoid glycosides (PEGs) in famous traditional Chinese medicine, Herba Cistanches. Though it has various bioactivities, such as antioxidation, neuroprotection and hepatoprotection, knowledge about its metabolic fate is scant. In the present study, eight phase II metabolites, 3, 4''''-*O*-dimethyl-ECH-3''''-*O*-*β*-D-glucuronide (M1), 4, 4''''-*O*-dimethyl-ECH-3''''-*O*-*β*-D-glucuronide (M2), 3, 4''''-*O*-dimethyl-ECH-4-*O*-sulfate ester (M3), 4, 4''''-*O*-dimethyl-ECH-3-*O*-sulfate ester (M4), 3, 3''''-*O*-dimethyl-ECH (M5), 3, 4''''-*O*-dimethyl-ECH (M6), 4, 3''''-*O*-dimethyl-ECH (M7), 4, 4''''-*O*-dimethyl-ECH (M8), were isolated from rat bile sample after intravenous administration of ECH and identified by mass spectra and NMR spectroscopy including ^{1}H NMR, ^{13}C NMR, NOEDS and two-dimensional NMR (HSQC, HMBC, gCOSY and NOESY). Among them, M5-M8 were O-di-methylated conjugates; M1 and M2, M3 and M4 were O-dimethyl glucuronides and O-dimethyl sulfates, respectively. In the three types of metabolites of rat, the major metabolites were the methyl ethers and the glucuronides, while the sulfates were minor. The regioselectivity of conjugation for ECH and metabolic pathway of ECH were proposed, which gave an insight into the mechanism of ECH for its bioactivities in vivo.

Introduction

Phenylethanoid glycosides (PEGs), as a type of polyphenolic compounds, are widely distributed in different plant families and possess various pharmacological effects, such as antioxidant, anti-inflammation, anti-anoxia, immunomodulation, and so on. Echinacoside (ECH; [(2R,3R,4R,5R,6R)-6-[2-(3,4-dihydroxyphenyl)ethoxy]-5-hydroxy-2-[[(2R,3R,4S, 5S,6R)-3,4,5-trihydroxy-6-(hydroxymethyl)oxan-2-yl]oxymethyl]-4-[(2S,3R,4R,5R,6S)-3,4, 5-trihydroxy-6-methyloxan-2-yl]oxyoan-3-yl](E)-3-(3,4-dihydroxyphenyl)prop-2-enoate) is one of the representative and major PEGs in Herba Cistanches (Tu, et al., 1997), which is an important traditional Chinese medicine used for the treatment of kidney deficiency and neurodegenerative diseases. ECH is also the main phenolic component in *Echinacea angustifolia* and *E. pallida* roots (Perry et al., 2001), which are widely used in Europe, North America and Australia for their immunostimulating activities. As a natural polyphenolic compound, ECH showed various bioactivities, such as antioxidative (Cervellati et al., 2002; Hu and Kitts, 2000; Xiong et al, 1996; Li et al., 1992), neuroprotective (Den et al., 2004; Koo et al., 2005; Chen et al., 2007; Geng et al., 2007), NO radical-scavenging (Xiong et al., 2000) and anti-hepatotoxic activities (Houghton and Hikino, 1989; Wu et al., 2007), et al.

Though ECH exhibited diverse bioactivities in in vivo and in vitro assays, only a few reports dealing with the metabolism and disposition of ECH are available. In our previous study on the pharmacokinetics and bioavailability of ECH in rat, the distribution and elimination of ECH were extremely fast in rat ($T_{1/2\alpha}$, 12.4 min; $T_{1/2\beta}$, 41.0 min) and CL was 0.0001 mg/kg/min/(ng/mL) after intraveneous administration (5 mg/kg), and the bioavailability of ECH was only 0.83% in rat (Jia et al., 2006). The very low bioavailability of

ECH was consistent with the result of Mattias' report, in which ECH permeated poorly through the Caco-2 monolayers (Mattias et al., 2004). Moreover, our pharmacokinetic data suggested that ECH was mostly metabolized after dosing. Therefore, we hypothesized that, in addition to the parent compound, some metabolic products of ECH may show biological activities, thereby contributing to the pharmacological efficacy of ECH in vivo. It was necessary to make the metabolic pathway of ECH clear to provide insight into the mechanism(s) through which it exerts its beneficial physiological effects.

As a follow-up study, we isolated and identified eight metabolites of ECH from rat bile.

Materials and Methods

Materials and chemicals. Echinacoside was separated and purified from an ethanol extract of *Cistanche tubulosa* (Schenk) R. Wight by our laboratory and its structure was confirmed by UV, IR, MS and NMR spectroscopy. The purity was 96.4% as determined by HPLC. HPLC grade acetonitrile was obtained from Caledon Laboratories LTD. (Georgetown, Ont., Canada). HPLC grade methanol was obtained from Concord Tech. (Tianjin, China). Trifluoroacetic acid was analytical grade. Water was glass-double distilled and filtered with 0.2 μm membranes. Macroporous resin D101 was purchased from the Chemical Plant of NanKai University (Tianjin, China). Sephadex LH-20 was the product of Pharmacia (Sweden). CD_3OD was obtained from Cambridge Isotope Laboratories, Inc. (Andover, MA).

Apparatus. Optical rotations were obtained on a PERKIN-ELMER 243B digital polarimeter. UV spectra were measured with a SHIMADZU spectrometer. IR spectra were determined using a NICOLET AVATAR 360 FTIR spectrometer. NMR spectra were recorded on Varian INOVA-500 NMR spectrometers equipped with 5 mm probes. About 10 mg sample was dissolved in 0.5 ml methanol-d_4 and transferred into a 5 mm NMR tube, which were measured by standard protocol at 298 K. ESI-MS were measured on a QSTAR mass spectrometer by mass scan in negative or positive ion mode. The HR-ESI-MS were measured on a Bruker APEX II FTCR spectrometer by mass scan in negative ion mode. Preparative HPLC was performed on a Waters model 600 instrument (Waters CO. Ltd., America; flow rate: 2.5ml/min; detective wavelength: UV 330 nm) with a Waters semi-preparative column (Prep. Nova-Pak HR C_{18}, 7.8 i.d.$\times$ 300 mm, 6 μm). Polyamide TLC plates were used in TLC analysis (Zhejiang Taizhou Sijia Bioplastic Plant). HPLC analysis was carried out on an

Agilent 1100 Series HPLC (Palo Alto, CA, USA) with UV detector. A C_{18} Symmetry Shield analytical column (4.6 i.d.× 250 mm, 5 μm, Waters CO. Ltd., America) protected by a C_{18} Security guard (4.0 mm × 3.0 mm, 5 μm, Phenomenex) was used. The column was maintained at 30˚C. The mobile phase consisted of solvent A (acetonitrile) and B (water containing 0.05% TFA). Gradient elution was as follows: initial 0-23 min, A-B (14.5:85.5, v/v); 23-28 min, linear change to A-B (16:84, v/v); 28-45 min, A-B (16:84, v/v); 45-46 min, linear change to A-B (14.5:85.5, v/v); 46-50 min, A-B (14.5:85.5, v/v). The flow rate was 1.0 mL/min. The ultraviolet (UV) detector was set at 330 nm.

Animals. Male Sprague-Dawley rats (290-310 g) were obtained from the Laboratory Animal Center of Peking University Health Science Center (Beijing, PR China). They were kept in an environmentally controlled animal room (temperature: 20 ± 2 ˚C, humidity: 60 ± 5%, 12 h dark/light cycle) for three days before starting the experiments and fed with standard laboratory food with water ad libitum and fasted overnight before the test.

Bile collection. Under light anesthesia with diethyl ether, bile fistulas in 12 rats were cannulated with PE-5 polyethylene tubing for collection of bile. The bile was collected into successive vials on ice at 2-h intervals for 8 h after dosing and at 8-12 h, 12-24 h, 24-30 h intervals thereafter. The rats were allowed to recover from anesthesia before receiving a 5 mg/kg intravenous dose of ECH in saline or 200 mg/kg oral dose of ECH in distilled water. During the period of bile collection, rats were kept in restraining cages with free access to water. All bile samples were stored at -30 ˚C until analysis.

Isolation of biliary metabolites. Bile was collected for 8 h from 20 rats with bile duct fistulae following bolus iv injection of 400 mg/kg ECH. The combined bile samples were

diluted 5-fold with water and subjected to a macroporous resin D101 column. The column

was eluted with water and 10% methanol (v/v) for 1000 ml consecutively, and then with

methanol for 2000 ml. The methanol elution was concentrated in vacuo to remove solvents,

and then the residue was dissolved in 50% methanol (v/v). The solution was subjected to

Sephadex LH-20 chromatogrphy and eluted with 50% methanol (v/v) to give three fractions

(Fr.1-3) with R_f 0.77, 0.15, 0.45 on polyamide TLC (MeOH/H$_2$O/HCOOH=15:35:0.5, freshly

prepared; blue spots after spraying with FeCl$_3$-K$_3$[Fe(CN)$_6$]), respectively. Fr.1-3 were

subjected to preparative HPLC [MeCN-0.05%TFA (16:84)] respectively. Fr.1 yielded M1 (25

mg, t_R = 19 min) and M2 (23 mg, t_R = 27 min); Fr.2 yielded M3 (15 mg, t_R = 12 min) and M4

(15 mg, t_R = 22 min); Fr.3 yielded M5 (18 mg, t_R = 42 min), M6 (63 mg, t_R = 48 min), M7 (12

mg, t_R = 56 min) and M8 (21 mg, t_R = 66 min). The purity of each metabolite was 91%, 90%,

96%, 95%, 96%, 93%, 96% and 95%, respectively, based on HPLC analyses.

Results

Isolation and structure elucidation of the eight metabolites. HPLC chromatography of

the bile samples from rats administrated ECH intravenously or orally revealed eight new large

peaks, named M1 to M8, showed in Fig.1B. The retention time of the eight metabolites was

longer than that of ECH, which was hardly detected. The retention time of ECH was about 9.7

min.

By the above methods, eight metabolites were obtained: M1 (25 mg), M2 (23 mg), M3

(15 mg), M4 (15 mg), M5 (18 mg), M6 (63 mg), M7 (12 mg), and M8 (21 mg). The structures

of them are shown in Fig.2.

Metabolite M6 (3, 4''''-*O*-dimethyl-ECH) was obtained as an amorphous light-yellowish

powder. Its HR-ESI-MS exhibited a pseudomolecular ion [M-H]$^-$ at *m/z* 813.2823. (calc. for

$C_{37}H_{49}O_{20}$, 813.2796), compatible with the molecular formula $C_{37}H_{50}O_{20}$. The IR spectrum

showed absorption bands typical of hydroxyls (3418 cm^{-1}), *α*, *β*-unsaturated ester (1678, 1631

cm^{-1}), and aromatic rings (1610, 1516 cm^{-1}). The ^{1}H NMR of M6 (Table 1) exhibited

characteristic proton signals of an *E*-caffeoyl group [three aromatic protons at *δ* 7.10 (*d*, *J*=2.0

Hz), 7.06 (*dd*, *J*=8.5, 2.0 Hz) and 6.92 (*d*, *J*=8.5 Hz) as an ABX system, two *trans* olefinic

protons as an AX system at *δ* 7.63 (*d*, *J*=16.0 Hz) and 6.34 (*d*, *J*=16.0 Hz)], a set of protons on

the 1, 3, 4-trisubstituted benzene ring [*δ* 6.85 (*d*, *J*=2.0 Hz), 6.72 (*d*, *J*=8.0 Hz) and 6.68 (*d*,

J=8.0, 2.0 Hz)], a triplet at *δ* 2.85 due to a *β*-methylene and two non-equivalent protons at *δ*

4.05 and 3.75 of the side chain of the aglycone moiety. Comparison of the ^{1}H and ^{13}C NMR

(Tables 1 and 2) data of M6 with those of ECH suggested that the structure of M6 is closely

related to that of ECH, except for two additional methoxyl groups. The location of the two

10

methoxyl groups at C-3 and C-4⁗ were inferred by the NOESY spectrum (Warashina et al.,

1992). In the NOESY spectrum, one methoxyl signal at δ 3.83 exhibited a NOE effect with

H-2 (δ 6.85), one of the aromatic protons in the aglycone moiety, and another methoxyl signal

at δ 3.86 showed a NOE effect with H-5⁗ (δ 6.92) in the ester moiety. On the basis of

spectral evidence, mainly 2D-NMR (HMBC and HSQC), the structure of M6 was elucidated

as 2-(3-methoxy-4-hydroxyphenyl)-ethyl *O*-α-L-rhamnopyranosyl-(1→3)-[*β*-D-glucopy-

ranosyl-(1→6)]-(4-*O*-*E*-isoferuloyl)-*β*-D-glucopyranoside.

Metabolite M5 (3, 3⁗-*O*-dimethyl-ECH) was also obtained as an amorphous

light-yellowish powder. The positive ESI-MS showed two pseudomolecular ion peaks at *m/z*

832.2 $[M+NH_4]^+$ and 837.2 $[M+Na]^+$, and the negative ESI-MS gave a pseudomolecular ion

peak at *m/z* 813.1 $[M-H]^-$, which corresponds to the molecular formula $C_{37}H_{50}O_{20}$ by

combining the ^1H and ^{13}C NMR data (Tables 1 and 2). On the basis of spectral evidence,

mainly 2D-NMR (HMBC and HSQC), the structure of M5, an isomer of M6, was elucidated

as cistanoside B, which was previously isolated from *Cistanche salsa* as a natural product

(Kobayashi et al., 1984).

Metabolite M7 (4, 3⁗-*O*-dimethyl-ECH) was also obtained as an amorphous

light-yellowish powder. The positive ESI-MS showed two pseudomolecular ion peaks at *m/z*

832.1 $[M+NH_4]^+$ and 837.1 $[M+Na]^+$, and the negative ESI-MS gave a pseudomolecular ion

peak at *m/z* 813.2 $[M-H]^-$, which corresponds to the molecular formula $C_{37}H_{50}O_{20}$ by

combining the ^1H and ^{13}C NMR data (Tables 1 and 2). By careful analysis of 2D-NMR

(HMBC and HSQC) spectral data, the structure of M7, an isomer of M6, was deduced as

2-(3-hydroxy-4-methoxyphenyl)-ethyl   *O*-α-L-rhamnopyranosyl-(1→3)-[*β*-D-glucopyranosyl-

(1→6)]-(4-*O*-*E*-feruloyl)-*β*-D-glucopyranoside, which was previously obtained from *Verbascum thapsus* as a natural product (Warashina et al., 1992).

Metabolite M8 (4, 4'''''-*O*-dimethyl-ECH) was also obtained as an amorphous light-yellowish powder. The positive ESI-MS showed a pseudomolecular ion peak at *m/z* 813.2 [M-H]⁻, which corresponds to the molecular formula $C_{37}H_{50}O_{20}$ by combining the ^{1}H and ^{13}C NMR data (Tables 1 and 2). By careful analysis of 2D-NMR (HMBC and HSQC) spectral data, the structure of M8, an isomer of M6, was deduced as 2-(3-hydroxy-4-methoxyphenyl)-ethyl *O*-*α*-L-rhamnopyranosyl-(1→3)-[*β*-D-glucopyranosyl-(1→6)]-(4-*O*-*E*-isoferuloyl)-*β*-D-glucopyranoside, which has been isolated from *Verbascum sinaiticum* as a natural product (Elgindi et al., 2000).

Metabolite M1 (3, 4'''''-*O*-dimethyl-ECH-3'''''-*O*-*β*-D-glucuronide): amorphous light-yellowish powder. Its HR-ESI-MS exhibited a pseudomolecular ion [M-H]⁻ at *m/z* 989.3143 (calc. for $C_{43}H_{57}O_{26}$, 989.3144), compatible with the molecular formula $C_{43}H_{58}O_{26}$. The IR spectrum showed absorption bands typical of hydroxyls (3414 cm⁻¹), *α*, *β*-unsaturated ester (1709, 1630 cm⁻¹), and aromatic rings (1604, 1515 cm⁻¹). Comparison of the ^{1}H and ^{13}C NMR data of M1 with those of M6 suggested that they are identical except that M1 has an additional glucuronide group, which was further supported by M1 having 176 mass units more than M6. Meanwhile, the ^{13}C NMR data clearly showed the existence of a glucuronic acid [*δ* 73.1 (C-4'''''), *δ* 74.7 (C-2'''''), *δ* 76.5 (C-5'''''), *δ* 77.3 (C-3'''''), *δ* 102.9 (C-1'''''), *δ* 173.6 (C-6''''')]. In the HMBC spectrum, the anomeric proton of glucuronide (*δ* 4.93, 1H, d, *J* = 8.0 Hz) had correlation with C-3'''' (*δ* 147.9), which indicated that the linkage site of glucuronic acid moiety was at C-3''''. The *β*-form anomeric configuration of the glucuronic

acid was judged from its coupling constant of the anomeric proton (J = 8.0 Hz). Furthermore,

the position of two methoxy groups at C-3 and C-4'''' was confirmed by an NOE experiment

where the OCH$_3$ resonances at δ 3.79 and δ 3.83 were irradiated. The resulting NOE

difference spectrum showed an enhancement of aromatic protons at δ 6.81 (H-2) and δ 6.98

(H-5''''), respectively. On the basis of spectral evidence, mainly 2D-NMR (HSQC, HMBC,

gCOSY), the structure of compound M1 was elucidated as

2-(3-methoxy-4-hydroxyphenyl)-ethyl O-α-L-rhamnopyranosyl-(1→3)-[β-D-glucopyranosyl-

(1→6)]-{4-[(2E)-3-(3-O-β-D-glucuronic acid-4-methoxy-phenyl)-2-propenoate]}-β-D-

glucopyranoside.

Metabolite M2 (4, 4''''-O-dimethyl-ECH-3''''-O-β-D-glucuronide): amorphous

light-yellowish powder. Its HR-ESI-MS exhibited a pseudomolecular ion [M-H]$^-$ at m/z

989.3147 (calc. for $C_{43}H_{57}O_{26}$, 989.3144), compatible with the molecular formula $C_{43}H_{58}O_{26}$.

The IR spectrum showed absorption bands typical of hydroxyls (3415 cm^{-1}), α, β-unsaturated

ester (1710, 1630 cm^{-1}), and aromatic rings (1602, 1514 cm^{-1}). M2 was 176 mass units higher

than that of M8, suggesting that it was a glucuronide conjugate of M8. Meanwhile, the ^{13}C

NMR data clearly showed the existence of a glucuronic acid [δ 73.0 (C-4''''''), δ 74.6 (C-2''''''),

δ 76.5 (C-5''''''), δ 77.3 (C-3''''''), δ 102.9 (C-1''''''), δ 173.3 (C-6'''''')]. In the HMBC spectrum,

the anomeric proton of glucuronide (δ 4.94, 1H, d, J = 7.5 Hz) had correlation with C-3'''' (δ

147.9), which indicated that the linkage site of glucuronic acid moiety was at C-3''''. The

β-form anomeric configuration of the glucuronic acid was judged from its coupling constant

of the anomeric proton (J = 7.5 Hz). Furthermore, the position of two methoxy groups at C-4

and C-4'''' was confirmed by an NOE experiment where the OCH$_3$ resonances at δ 3.75 and δ

13

3.83 were irradiated. The resulting NOE difference spectrum showed an enhancement of aromatic protons at δ 6.77 (H-5) and δ 6.98 (H-5''''), respectively. On the basis of spectral evidence, mainly 2D-NMR (HSQC, HMBC, gCOSY), the structure of compound M2 was elucidated as 2-(3-hydroxy-4-methoxyphenyl)-ethyl *O*-α-L-rhamnopyranosyl-(1→3)-[β-D-glucopyranosyl-(1→6)]-{4-[(2*E*)-3-(3-O-β-D-glucuronic acid-4-methoxy-phenyl)-2-propenoate]}-β-D-glucopyranoside.

Metabolite M3 (3, 4''''-*O*-dimethyl-ECH-4-*O*-sulfate ester): amorphous light-yellowish powder. Its HR-ESI-MS showed the pseudomolecular ion [M-H]$^-$ at *m/z* 893.2337 (calc. for $C_{37}H_{49}O_{23}S$, 893.2391). The molecular formula was determined to be $C_{37}H_{50}O_{23}S$ in combination with the ^{1}H and ^{13}C NMR spectral data. The presence of a sulfate moiety was deduced by the appearance of intense distinctive absorption bands at 1268, 1045 cm^{-1} in the IR spectrum of **M3**, which was ascribed to the conjugated S-O bond stretching vibration. The IR spectrum also showed absorption bands typical of hydroxyls (3428 cm^{-1}), α, β-unsaturated ester (1700, 1630 cm^{-1}), aromatic rings (1609, 1512 cm^{-1}). The molecular formula of M3 was 80 mass units higher than that of M6, suggesting that M3 was a sulfate conjugate of M6. The ^{13}C NMR data of M3 were similar to M6, except for the downfield shifts of C-3 (+4.3 ppm) and C-5 (+7.5 ppm), and the upfield shifts of C-4 (-4.6 ppm), which showed that the sulfonate group was linked at C-4. On the basis of spectral evidence, mainly 2D-NMR (HSQC, HMBC), the structure of compound M3 was elucidated as 2-(3-methoxy-4-sulfophenyl)-ethyl *O*-α-L-rhamnopyranosyl-(1→3)-[β-D-glucopyranosyl-(1→6)]-(4-*O*-*E*-isoferuloyl)-β-D-glucopyranoside.

Metabolite M4 (4, 4''''-*O*-dimethyl-ECH-3-*O*-sulfate ester): amorphous light-yellowish

powder. Its HR-ESI-MS exhibited a pseudomolecular ion [M-H]$^-$ at *m/z* 893.2348 (calc. for

$C_{37}H_{49}O_{23}S$, 893.2391). The molecular formula was determined to be $C_{37}H_{50}O_{23}S$ in

combination with the ^{1}H and ^{13}C NMR spectral data. The presence of a sulfate moiety was

deduced by the appearance of intense distinctive absorption bands at 1267, 1046 cm^{-1} in the

IR spectrum of **M4**, which was ascribed to the conjugated S-O bond stretching vibration. The

IR spectrum also showed absorption bands typical of hydroxyls (3428 cm^{-1}), *α, β*-unsaturated

ester (1702, 1630 cm^{-1}), aromatic rings (1611, 1514 cm^{-1}). The molecular formula of M4 was

80 mass units higher than that of M8, suggesting that M4 was a sulfate conjugate of M8. The

^{13}C NMR data of M4 were similar to M8, except for the downfield shifts of C-2 (+7.4 ppm)

and C-4 (+4.1 ppm), and the upfield shifts of C-3 (-4.7 ppm), which showed that the sulfonate

group was linked at C-3. On the basis of spectral evidence, mainly 2D-NMR (HSQC, HMBC),

the structure of compound **M4** was elucidated as 2-(3-sulfo-4-methoxyphenyl)-ethyl

O-α-L-rhamnopyranosyl-(1→3)-[*β*-D-glucopyranosyl-(1→6)]-(4-*O-E*-isoferuloyl)-*β*-D-

glucopyranoside.

Discussion

During the drug metabolism studies, it becomes vitally important to identify and characterize the structure of metabolites. In recent years, new techniques were applied to identify and characterize the metabolites, such as GC/MS, LC/MS (Corinna et al., 2006; Xu et al., 2006), LC/NMR (Mutlib AE and Shockcor JP, 2003), NMR (Zhang et al., 2004; Zeng et al., 2007) and stable isotopes. In our study, three groups of positional isomers (M5, M6, M7 and M8; M1 and M2; M3 and M4) were obtained. It was very difficult to identify the structure of these metabolites only by LC/MS^n data. So preparation of metabolites and further identification based on NMR data must be done. Of course, the direct isolation of the metabolites from bile, urine, or feces of humans or other animals was a tedious and laborious task, but it is the most reliable method in the identification of metabolites.

We have reported the low bioavailability (0.83%) of ECH in rat after oral administration (Jia et al., 2006). The extremely low bioavailability was mainly due to poor absorption of ECH through the gastrointestinal tract. In the present study, we have firstly investigated the metabolites of ECH from rat bile. Eight metabolites of ECH were isolated and identified by mass spectra, IR and NMR spectroscopy including ^{1}H NMR, ^{13}C NMR, NOEDS and two-dimensional NMR (HMQC, HMBC, gCOSY, and NOESY). All of the eight metabolites were phase II metabolites. Among them, M5-M8 were O-dimethyl conjugates; M1 and M2, M3 and M4 were O-dimethyl glucuronides and O-dimethyl sulfates, respectively.

Few reports about the metabolism of PEGs can be found. Our group previously reported ECH was hydrolyzed to acteoside by enzymes of bacterial origin in the large intestine of beagle dogs (Lei et al., 2001). In the present study, three types of metabolic pathway for ECH

in rats were revealed (Shown in Fig. 2). One was the methylation of the phenolic hydroxyl groups in the ester and aglycone for ECH and four positional isomeric O-dimethyl metabolites were formed. Interestingly, the monomethyl metabolites were not isolated and identified, which suggested that phenolic hydroxyls on ester or aglycon are easy to be methylated and the catechol is hardly to be methylated simultaneously. The second was that the glucuronidation tends to occur on hydroxyl groups of the ester moiety in ECH. Two isomeric O-dimethyl glucuronides were formed. The third was that the sulfation tends to occur on hydroxyl groups of the aglycone moiety in ECH. Two O-dimethyl sulfates were identified. In addition, the author also studied the metabolism of ECH in the gut and the serum in rat. Two metabolites were detected in the gut. And they were identified as acteoside and caffeic acid based on their retention times as compared with authentic standards and on LC-MS (ESI-MS/MS) analyses.

It was previously reported that the preferential conjugation sites existed in the conjugate formation for flavonoid compounds (Morand et al., 1998; Boersma et al., 2002; Havsteen, 2002; Chen et al., 2006; Bursztyka et al., 2007) and caffeic acid and its oligomer condensate (Moridani et al., 2002, Zhang et al., 2004). In the present study, the preferential conjugation sites also existed in the conjugate formation for ECH, which may be related to the steric configuration of the ECH or COMT, UGT, and ST (species difference). Of the three types of metabolites in rat, the major conjugates were the methyl ethers and the glucuronides, while the sulfates were minor. Among four methyl ethers, the content of M6 was larger than others by comparing their peak area in HPLC chromatogram, which revealed the possibilities of the methylation on 4''''-OH and 3-OH in ECH at the same time was larger than that of other

hydroxyls. Furthermore, the glucuronidation with a high selectivity only occurred on the 3''''-OH group of the ester. So the 3''''-OH group of the ester of ECH was determined as the preferential site for glucuronosyl conjugation compared with other three hydroxyl groups. Moreover, sulfate ester formation occurred at hydroxyl 3 or 4 of the aglycone, while the ester contained 3''''-OH and 4''''-OCH$_3$. However, the conjugates with mixed methylates/sulfates/glucuronides or sulfate/glucuronides were not found. Further studies should clarify whether they were formed or not.

Metabolism of ECH involves methylation by the enzyme COMT, glucuronidation by the enzyme UGT and sulfation by ST in the liver. COMT is an intracellular enzyme, widely distributed throughout the organs of the body with the highest COMT activity is in the liver, followed by the kidneys and gastrointestinal tract (Karhunen et al., 1994). Some phenolic compounds, such as caffeic acid (Moridani et al., 2002), quercetin (O'Leary et al., 2003), magnesium lithospermate B (Zhang et al., 2004), and so on, were reported to be methelated in the catechol moiety by COMT. In the present study, ECH were methylated in the catechol moiety at the 3'''', 4''''-OH of the ester and at the 3-, 4-OH of the aglycone, to form four O-di-methylated conjugates (M5, M6, M7, and M8), respectively, by COMT. Additionally, glucuronidation and sulfation reactions, may well be a major cause for the lack of toxicity of phenolic compounds (Morand et al., 1998), and seemed to be the other major metabolic pathways to biotransform catechols into conjugates unable to enter a redox cycling reaction for phenolic compounds (Bursztyka et al., 2007). Two O-dimethyl glucuronides and two O-dimethyl sulfates were also identified in the present study, respectively. Moreover, the glucuronidation and sulfadation improves the water solubility of methoxylated derivatives of

ECH and consequently favors their elimination. Further study on metabolism need to be investigated and identified the enzymes involved in the formation of metabolites of ECH.

In summary, eight phase II metabolites have been isolated and identified from bile collected from rats after oral or intraveneous administration of ECH, and four of them were O-dimethyl conjugates, two O-dimethyl glucuronides, two O-dimethyl sulfates. The methylation and glucuronidation conjugates were major metabolites while sulfation conjugates were minor. The hydroxyl groups of the aglycone and the ester could also be methylated. The preferential site for the glucuronidation was 3''''-OH of the ester and the preferential sites for sulfation were 3 or 4-OH of the aglycone. All above results are important for the understanding of ECH metabolism in rats and provide information and reference for the further metabolic investigation of ECH in humans.

Supplemental data:

Supplement Data Available: MS, IR, 1D and 2D NMR spectra of M1-M8 in CD_3OD.

Reference

Boersma MG, van der Woude H, Bogaards J, Boeren S, Vervoort J, Cnubben NH, van Iersel ML, van Bladeren PJ, and Rietjens IM (2002) Regioselectivity of phase II metabolism of luteolin and quercetin by UDP-glucuronosyl transferases. *Chem Res Toxicol* **15**: 662-670.

Bursztyka J, Perdu E, Tulliez J, Debrauwer L, Delous G, Canlet C, Sousa GD, Rahmani R, Benfenati E, and Cravedi JP (2008) Comparion of genistein metabolism in rats and humans using liver microsomes and hepatocytes. *Food Chem Toxicol* **46**:939-948.

Cervellati R, Renzulli C, Guerra MC and Speroni E (2002) Evaluation of antioxidant activity of some natural polyphenolic compounds using the briggs-rauscher reaction method. *J Agric Food Chem* **50**:7504-7509.

Chen H, Jing FC, Li CL, Tu PF, Zheng QS, and Wang ZH (2007) Echinacoside prevents the striatal extracellular levels of monoamine neurotransmitters from diminution in 6-hydroxydopamine lesion rats. *J Ethnopharmacol* **114**:285-289.

Chen XY, Cui L, Duan XT, Ma B, and Zhong DF (2006) Pharmacokinetics and metabolism of the flavonoid scutellarin in humans after a single oral administration. *Drug Metab Dispos* **34**:1345-1352.

Den M, Zhao JY, Tu PF, Jiang Y, Li ZB, and Wang YH (2004) Echinacoside rescues the SHSY5Y neuronal cells from TNFα-induced apoptosis. *Eur J Pharmacol* **505**:11-18.

Elgindi MR, Mabry TJ (2000) Phenylethanoid glycosides from *Verbascum sinaiticum*. *Asian J Chem* **12**: 127-130.

Geng XC, Tian XF, Tu PF, and Pu XP (2007) Neuroprotective effects of echinacoside in the mouse MPTP model of Parkinson's disease. *Eur J Pharmacol* **564**:66-74.

Havsteen BH (2002) The biochemistry and medical significance of the flavonoids. *Pharmacol Ther* **96**:67-202.

Houghton PJ and Hikino H (1989) Anti-hepatotoxic activity of extracts and constituents of

Buddleja apecies. *Planta Med* **55**:123-126.

Hu C and Kitts DD (2000) Studies on the antioxidant activity of Echinacea root extract. *J Agric Food Chem* **48**:1466-1472.

Jia CQ, Shi HM, Wu XM, Li YZ, Chen JJ, and Tu PF (2006) Determination of echinacoside in rat serum by reversed-phase high-performance liquid chromatography with ultraviolet detection and its application to pharmacokinetics and bioavailability. *J Chromatogr B* **844**:308-313.

Jong H, Ihsan C, Hasan K, Wolfgang S, Sebnem H, and Otto S (2000). Radical scavenger activity of phenylethanoid glycosides in FMLP stimulated human polymorphonuclear leukocytes: structure-activity relationships. *Planta Med* **66**:746-748.

Karhunen T, Tilgmann C, Ulmanen I, Julkunen I, and Panula P (1994) Distribution of catechol-O-methyltransferase enzyme in rat tissues. *J Histochem Cytochem* **42**: 1079-1090.

Kobayashi H, Karasawa H, Miyase T, and Fukushima S (1984) Studies on the constituents of Cistanchis herba. Ⅲ. isolation and structures of new phenylpropanoid glycosides, cistanosides A and B. *Chem Pharm Bull* **32**:3009-3014.

Koo KA, Sung SH, Park JH, Kim SH, Lee KY, and Choong-Kim Y (2005) In vitro neuroprotective activities of phenylethanoid glycosides from Callicarpa dichotoma. *Planta Med* **71**:778-780.

Lei L, Song ZH, Tu PF, Li YZ, Wu LJ, and Chen FK(2001) Metabolic regulation of phenylethanoid glycosides from Herba cistanches in dogs' gastrointestine. *Acta Pharm Sin* **36**:432-435.

Li J, Zheng RL, Liu ZM, and Jia ZJ (1992) Scavenging effects of phenylpropanoid glycosides on superoxide and its antioxidation effect. *Acta Pharmacol Sin* **13**:427-430.

Matthias A, Blanchfield JT, Penman KG, Toth I, Lang CS, De Voss JJ, and Lehmann RP (2004), Permeability studies of alkylamides and caffeic acid conjugates from echinacea

using a Caco-2 cell monolayer model. *J Clin Pharm Therapeut* **29**:7-13.

Morand C, Crespy V, Manach C, Besson C, Demigné C, and Rémésy C (1998) Plasma metabolites of quercetin and their antioxidant properties. *Am J Physiol Regulatory Integrative Comp Physiol* **275**:212-219.

Moridani MY, Scobie H, and O'Brien PJ (2002) Metabolism of caffeic acid by isolated rat hepatocytes and subcellular fractions. *Toxicol Lett* **133**:141-151.

Mutlib AE and Shockcor JP (2003). Application of LC/MS, LC/NMR, NMR and stable isotopes in identifying and characterizing metabolites, in *Drug Metabolizing Enzymes* (Lee JS and Fisher MB eds) pp39-50, FontisMedia SA, Lausamme and Marcel Dekker, Inc., New York.

O'Leary KA, Day AJ, Needs PW, Mellon FA, O'Brien NM, and Williamson G (2003) Metabolism of quercetin-7- and quercetin-3-glucuronides by an *in vitro* hepatic model: the role of human β-glucuronidase, sulfotransferase, catechol-O-methyltransferase and multi-resistant protein 2 in flavonoid metabolism. *Biochem Pharmacol* **65**:479-491.

Perry NB, Burgess EJ, and Glennie VL (2001) Echinacea standardization: analytical methods for phenolic compounds and typical levels in medicinal species. *J Agric Food Chem* **49**: 1702-1706.

Rüfer CE, Glatt H, and Kulling SE (2006) Structure elucidation of hydroxylated metabolites of the isoflavan equol by gas chromatography-mass spectrometry and high performance liquid chromatography-mass spectrometry. *Drug Metab Dispos* **34**:51-60.

Tu PF, Wang B, Deyama T, Zhang ZG and Lou ZC (1997) Analysis of phenylethanoid glycoside of herba cistanchis by RP-HPLC. *Acta Pharm Sin* **32**:294-300.

Warashina T, Miyase T, and Ueno A (1992) Phenylethnoid and lignan glycosides from *Verbascum thapsus*. *Phytochemistry* **31**:961-965.

Wen X and Walle T (2006) Methylated flavonoids have greatly improved intestinal absorption

and metabolic stability. *Drug Metab Dispos* **34**:1786-1792.

Wu Y, Li L, Wen T, and Li YQ (2007) Protective effects of echinacoside on carbon tetrachloride-induced hepatotoxicity in rats. *Toxicology* **232**:50-56.

Xiong Q, Tezuka Y, Kaneko T, Li H, Tran LQ, Hase K, Namba T, and Kadota S (2000) Inhibition of nitric oxide by phenylethanoids in activated macrophages. *Eur J Pharmacol* **400**:137-144.

Xiong QB, Kadota S, Tani T, and Namba T (1996) Antioxidative effects of phenylethanoids from *Cistanche deserticola*. *Biol Pharm Bull* **19**:1580-1585.

Xu F, Zhang Y, Xiao SY, Lu XW, Yang DH, Yang XD, Li CL, Shang MY, Tu PF, and Cai SQ (2006) Absorption and metabolism of Astragali Radix decoction: in silico, in vitro, and a case study in vivo. *Drug Metab Dispos* **34**:913-924.

Zeng YC, Qiu F, Liu Y, Qu GX, and Yao XS (2007) Isolation and identification of phase 1 metabolites of demethoxycurcumin in rats. *Drug Metab Dispos* **35**:1564-1573.

Zhang Y, Akao T, Nakamura N, Hattori M, Yang XW, Duan CL, and Liu JX (2005) Magnesium lithospermate B is excreted rapidly into rat bile mostly as methylated metabolites, which are potent antioxidants. *Drug Metab Dispos* **32**:752-757.

Footnotes:

Legends for figures

Fig.1 Typical chromatograms of blank bile (A); a bile sample during 4-6 h after an i.g. dose of

200 mg/kg of ECH (B).

Fig.2 Proposed metabolic pathways of ECH

Tables

Table 1. ^{1}H-NMR Data for Metabolites M5-M8 (δ in ppm, J in Hz)

No.	M5	M6	M7	M8	Echinacoside
Aglycone					
2	6.86 (*d*, 1.5)	6.85 (*d*, 2.0)	6.74 (*d*, 2.0)	6.74 (*d*, 2.0)	6.65 (*d*, 2.0)
5	6.70 (*m*)	6.72 (*d*, 8.0)	6.81 (*d*, 8.0)	6.82 (*d*, 8.5)	6.62 (*d*, 8.0)
6	6.69 (*m*)	6.68 (*d*, 8.0, 2.0)	6.69 (*d*, 8.0, 2.0)	6.69 (*d*, 8.5, 2.0)	6.52 (*d*, 8.0, 2.0)
α	4.06 (*m*), 3.76 (*m*)	4.05 (*m*), 3.75 (*m*)	4.05 (*m*), 3.74 (*m*)	4.05 (*m*), 3.74 (*m*)	3.98 (*m*), 3.66 (*m*)
β	2.85 (*m*)	2.85 (*m*)	2.82 (*m*)	2.82 (*m*)	2.74 (*m*)
Inner glucose					
1′	4.40 (*d*, 8.0)	4.40 (*d*, 8.0)	4.39 (*d*, 8.0)	4.39 (*d*, 8.0)	4.33 (*d*, 8.0)
2′	3.40 (*m*)	3.41 (*m*)	3.39 (*m*)	3.39 (*m*)	3.33 (*m*)
3′	3.82 (*m*)	3.82 (*m*)	3.81 (*m*)	3.81 (*m*)	3.75 (*m*)
4′	5.01 (*t*, 9.5)	5.03 (*t*, 9.5)	5.00 (*t*, 9.5)	5.00 (*t*, 9.5)	4.95 (*t*, 9.5)
5′	3.76 (*m*)	3.76 (*m*)	3.76 (*m*)	3.77 (*m*)	3.70 (*m*)
6′	3.95 (*m*), 3.62 (*m*)	3.95 (*m*), 3.62 (*m*)	3.94 (*m*), 3.64 (*m*)	3.94 (*m*), 3.64 (*m*)	3.89 (*m*), 3.58 (*m*)
Rhamnose					
1″	5.19 (*br.s*)	5.19 (*br.s*)	5.19 (*br.s*)	5.18 (*d*, 1.5)	5.12 (*br.s*)
2″	3.57 (*m*)	3.58 (*m*)	3.56 (*m*)	3.56 (*m*)	3.51 (*m*)
3″	3.91 (*m*)	3.94 (*m*)	3.91 (*m*)	3.92 (*m*)	3.87 (*m*)
4″	3.28 (*m*)	3.30 (*m*)	3.29 (*m*)	3.28 (*m*)	3.23 (*m*)
5″	3.57 (*m*)	3.55 (*m*)	3.56 (*m*)	3.54 (*m*)	3.50 (*m*)
6″	1.09 (*d*, 6.0)	1.08 (*d*, 6.5)	1.08 (*d*, 6.0)	1.07 (*d*, 6.0)	1.02 (*d*, 6.0)
Outer glucose					
1‴	4.28 (*d*, 8.0)	4.28 (*d*, 7.5)	4.29 (*d*, 7.5)	4.29 (*d*, 8.0)	4.24 (*d*, 7.5)
2‴	3.19 (*m*)	3.21 (*m*)	3.19 (*m*)	3.20 (*m*)	3.14 (*m*)
3‴	3.31 (*m*)	3.34 (*m*)	3.32 (*m*)	3.32 (*m*)	3.28 (*m*)
4‴	3.26 (*m*)	3.28 (*m*)	3.26 (*m*)	3.26 (*m*)	3.21 (*m*)
5‴	3.21 (*m*)	3.22 (*m*)	3.21 (*m*)	3.22 (*m*)	3.17 (*m*)
6‴	3.82 (*m*), 3.62 (*m*)	3.82 (*m*), 3.63 (*m*)	3.82 (*m*), 3.62 (*m*)	3.82 (*m*), 3.62 (*m*)	3.77 (*m*), 3.55 (*m*)
Ester					
2⁗	7.18 (*d*, 1.5)	7.10 (*d*, 2.0)	7.20 (*d*, 1.5)	7.08 (*d*, 2.0)	7.00 (*d*, 2.0)
5⁗	6.79 (*d*, 8.0)	6.92 (*d*, 8.5)	6.82 (*d*, 7.5)	6.94 (*d*, 7.5)	6.72 (*d*, 8.0)
6⁗	7.07 (*dd*, 8.0, 1.5)	7.06 (*dd*, 8.5, 2.0)	7.08 (*dd*, 7.5, 1.5)	7.06 (*dd*, 7.5, 2.0)	6.90 (*dd*, 8.0, 2.0)
α′	6.35 (*d*, 15.5)	6.34 (*d*, 16.0)	6.37 (*d*, 16.0)	6.32 (*d*, 16.0)	6.22 (*d*, 15.5)
β′	7.66 (*d*, 15.5)	7.63 (*d*, 16.0)	7.66 (*d*, 16.0)	7.62 (*d*, 16.0)	7.54 (*d*, 15.5)
3-OCH$_3$	3.84 (s)	3.83 (s)			
4-OCH$_3$			3.81 (s)	3.81 (s)	
3⁗-OCH$_3$	3.87 (s)		3.89 (s)		
4⁗-OCH$_3$		3.86 (s)		3.88 (s)	

[a] All spectra were recorded on a Varian INOVA-500 spectrometer, in CD$_3$OD.

[b] m, multiple split.

[c] br.s, broad singlet.

Table2. ^{13}C-NMR Data for Metabolites M1-M8 (δ in ppm)

No.	M1	M2	M3	M4	M5	M6	M7	M8	Echinacoside
Aglycone									
1	131.6	132.9	138.0	132.5	131.6	131.5	132.9	132.9	131.4
2	113.8	117.1	115.0	124.5	113.8	113.7	117.1	117.1	116.5
3	148.8	147.3	153.0	142.6	148.8	148.7	147.3	147.3	146.1
4	145.9	147.5	141.2	151.7	145.9	145.8	147.5	147.6	144.5
5	116.1	112.9	123.6	112.5	116.1	116.1	112.9	112.9	117.1
6	122.4	121.2	121.9	127.1	122.4	122.4	121.2	121.2	121.3
α	72.3	72.2	71.9	72.0	72.3	72.2	72.2	72.2	72.3
β	36.7	36.5	36.9	36.4	36.7	36.6	36.5	36.5	36.6
Inner glucose									
1'	104.2	104.2	104.1	104.2	104.2	104.1	104.2	104.2	104.1
2'	76.1	76.1	76.1	76.1	76.2	76.0	76.1	76.1	76.1
3'	81.3	81.4	81.7	81.8	81.5	81.6	81.5	81.6	81.6
4'	70.8	70.8	70.7	70.7	70.6	70.6	70.6	70.7	70.5
5'	74.6	74.6	74.7	74.7	74.7	74.5	74.8	74.7	74.7
6'	69.4	69.4	69.4	69.4	69.4	69.3	69.4	69.4	69.4
Rhamnose									
1″	102.9	102.9	103.1	103.1	103.0	103.0	103.0	103.1	103.1
2″	72.1	72.1	72.0	72.0	72.1	72.0	72.1	72.0	71.9
3″	72.3	72.3	72.3	72.3	72.3	72.2	72.3	72.3	72.4
4″	73.7	73.7	73.7	73.8	73.8	73.7	73.7	73.7	73.7
5″	70.4	70.4	70.4	70.4	70.4	70.4	70.4	70.4	70.4
6″	18.5	18.5	18.4	18.5	18.4	18.4	18.4	18.4	18.4
Outer glucose									
1‴	104.6	104.6	104.7	104.7	104.7	104.5	104.7	104.7	104.6
2‴	75.1	75.1	75.1	75.1	75.1	75.0	75.1	75.1	75.1
3‴	77.8	77.8	77.8	77.8	77.8	77.7	77.8	77.8	77.8
4‴	71.5	71.4	71.5	71.5	71.5	71.3	71.5	71.4	71.4
5‴	77.9	77.9	77.9	77.9	77.9	77.8	77.9	77.9	77.9
6‴	62.7	62.7	62.6	62.6	62.6	62.5	62.6	62.6	62.6
Ester									
1⁗	128.7	128.7	128.8	128.8	127.1	128.7	127.6	128.8	127.6
2⁗	117.9	117.9	114.9	114.9	111.7	114.8	111.8	114.9	114.6
3⁗	147.9	147.9	148.0	148.0	151.8	147.8	150.9	148.1	146.8
4⁗	153.6	153.6	151.7	151.7	149.6	151.6	149.4	151.7	149.6
5⁗	113.5	113.6	112.5	112.5	116.7	112.5	116.5	112.5	116.3
6⁗	126.0	126.1	123.1	123.1	124.6	123.1	124.4	123.1	123.3
α'	116.5	116.5	115.8	115.8	114.7	115.7	115.1	115.7	115.2
β'	147.3	147.3	147.8	147.8	148.3	147.8	148.1	147.8	148.2
C=O	168.2	168.2	168.3	168.3	168.5	168.3	168.4	168.3	168.4
Glucuronic acid									

1‴‴	102.9	102.9	–	–	–	–	–	–
2‴‴	74.7	74.6	–	–	–	–	–	–
3‴‴	77.3	77.3	–	–	–	–	–	–
4‴‴	73.1	73.0	–	–	–	–	–	–
5‴‴	76.5	76.5	–	–	–	–	–	–
6‴‴	173.6	173.3	–	–	–	–	–	–
3-OCH$_3$	56.5	–	56.7	–	56.5	56.5	–	–
4-OCH$_3$	–	56.5	–	56.8	–	–	56.5	56.5
3‴′-OCH$_3$	–	–	–	–	56.4	–	56.5	–
4‴′-OCH$_3$	56.7	56.7	56.4	56.4	–	56.4	–	56.4

Table 3. ^{1}H-NMR Data for Metabolites M1-M4 (δ in ppm, J in Hz)

No.	M1	M2	M3	M4
Aglycone				
2	6.81 (*d*, 1.5)	7.39 (*d*, 2.0)	6.92 (*d*, 2.0)	7.39 (*d*, 2.0)
5	6.65 (*m*)	6.89 (*d*, 8.0)	7.29 (*d*, 8.0)	6.89 (*d*, 8.0)
6	6.64 (*m*)	6.98 (*dd*, 8.0, 2.0)	6.76 (*dd*, 8.0, 2.0)	6.98 (*dd*, 8.0, 2.0)
α	4.02 (*m*), 3.72 (*m*)	4.00 (*m*), 3.70 (*m*)	4.04 (*m*), 3.76 (*m*)	4.03 (*m*), 3.72 (*m*)
β	2.80 (*m*)	2.77 (*m*)	2.87 (*m*)	2.82 (*m*)
Inner glucose				
1'	4.35 (*d*, 8.0)	4.33 (*d*, 8.0)	4.36 (*d*, 7.5)	4.33 (*d*, 8.0)
2'	3.35 (*m*)	3.36 (*m*)	3.34 (*m*)	3.35 (*m*)
3'	3.78 (*m*)	3.78 (*m*)	3.77 (*m*)	3.75 (*m*)
4'	4.96 (*m*)	4.96 (*m*)	4.95 (*t*, 9.5)	4.94 (*t*, 9.5)
5'	3.72 (*m*)	3.73 (*m*)	3.72 (*m*)	3.72 (*m*)
6'	3.89 (*m*), 3.58 (*m*)	3.88 (*m*), 3.59 (*m*)	3.87 (*m*), 3.59 (*m*)	3.88 (*m*), 3.58 (*m*)
Rhamnose				
1''	5.15 (*br.s*)	5.13 (*br.s*)	5.13 (*br.s*)	5.13 (*br.s*)
2''	3.53 (*m*)	3.52 (*m*)	3.52 (*m*)	3.52 (*m*)
3''	3.86 (*m*)	3.86 (*m*)	3.86 (*m*)	3.88 (*m*)
4''	3.24 (*m*)	3.24 (*m*)	3.24 (*m*)	3.24 (*m*)
5''	3.51 (*m*)	3.50 (*m*)	3.49 (*m*)	3.49 (*m*)
6''	1.03 (*d*, 6.0)	1.03 (*d*, 6.0)	1.02 (*d*, 6.0)	1.01 (*d*, 5.5)
Outer glucose				
1'''	4.23 (*d*, 7.0)	4.25 (*d*, 8.0)	4.24 (*d*, 8.0)	4.25 (*d*, 8.0)
2'''	3.15 (*m*)	3.16 (*m*)	3.15 (*m*)	3.16 (*m*)
3'''	3.28 (*m*)	3.29 (*m*)	3.27 (*m*)	3.28 (*m*)
4'''	3.22 (*m*)	3.22 (*m*)	3.22 (*m*)	3.22 (*m*)
5'''	3.16 (*m*)	3.17 (*m*)	3.16 (*m*)	3.17 (*m*)
6'''	3.76 (*m*), 3.57 (*m*)	3.76 (*m*), 3.58 (*m*)	3.78 (*m*), 3.59 (*m*)	3.76 (*m*), 3.59 (*m*)
Ester				
2''''	7.40 (*d*, 2.0)	7.03 (*d*, 2.0)	7.03 (*d*, 2.0)	7.03 (*d*, 2.0)
5''''	6.98 (*d*, 7.5)	6.89 (*d*, 8.0)	6.89 (*d*, 8.0)	6.89 (*d*, 8.0)
6''''	7.24 (*dd*, 7.5, 2.0)	7.02 (*dd*, 8.0, 2.0)	7.02 (*dd*, 8.0, 2.0)	7.02 (*dd*, 8.0, 2.0)
α'	6.35 (*d*, 15.5)	6.27 (*d*, 15.5)	6.28 (*d*, 15.5)	6.27 (*d*, 15.5)
β'	7.61 (*d*, 15.5)	7.57 (*d*, 15.5)	7.57 (*d*, 15.5)	7.57 (*d*, 15.5)
Glucuronic acid				
1'''''	4.93 (*d*, 8.0)	4.94 (*d*, 7.5)	–	–
2'''''	3.52 (*m*)	3.51 (*m*)	–	–
3'''''	3.48 (*m*)	3.48 (*m*)	–	–
4'''''	3.56 (*m*)	3.58 (*m*)	–	–
5'''''	3.85 (*m*)	3.86 (*m*)	–	–
3-OCH$_3$	3.79 (s)	–	3.78 (s)	–
4-OCH$_3$	–	3.75 (s)	–	3.75 (s)
3''''-OCH$_3$	–	–	–	–

4′′′′′-OCH$_3$	3.83 (s)	3.83 (s)	3.83 (s)	3.83 (s)

^{a} All spectra were recorded on a Varian INOVA-500 spectrometer, in CD$_3$OD.
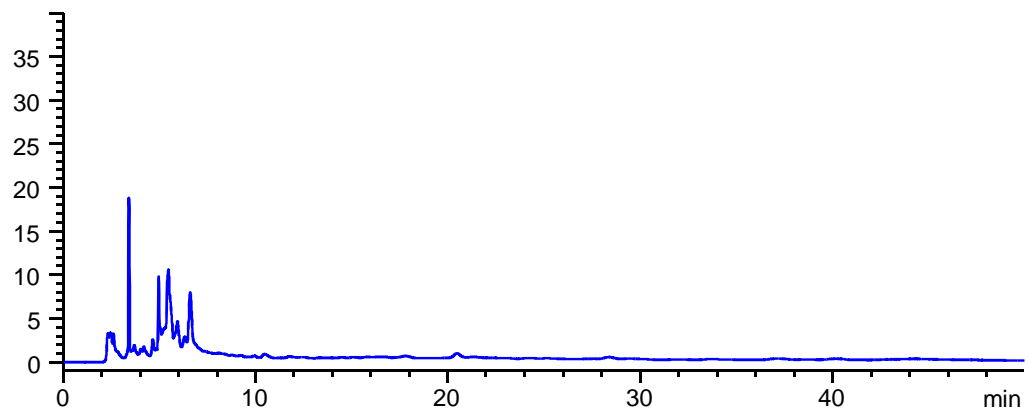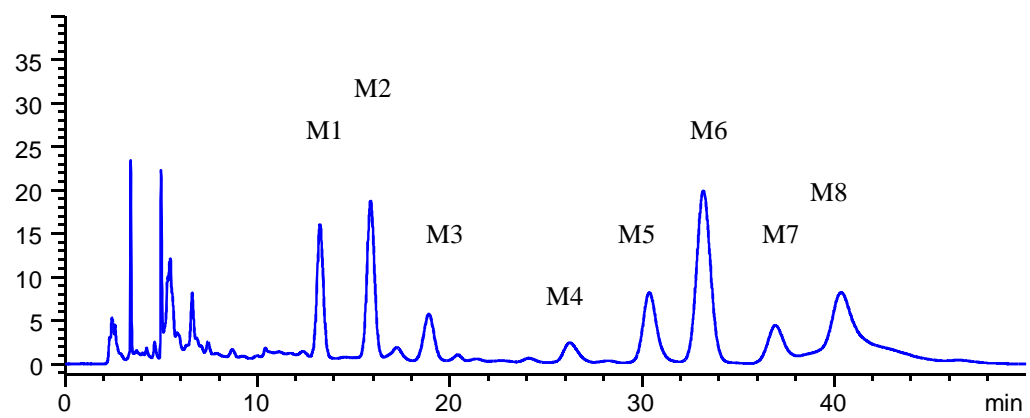
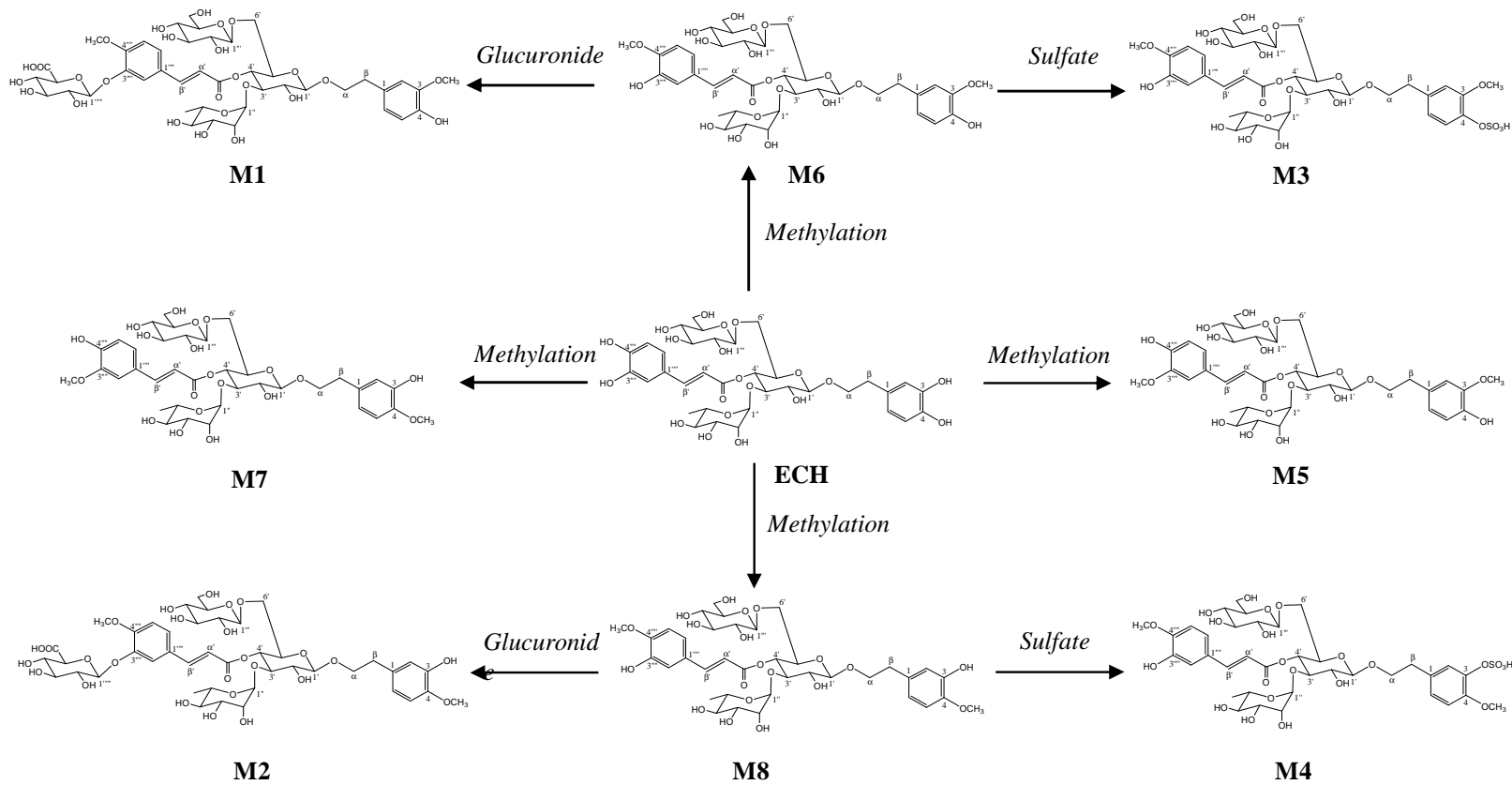^{b} m, multiple split.

^{c} br.s, broad singlet.

Figure 1A

Figure 1B

Fig.2 Proposed metabolic pathways of ECH